Volume 60 http://acousticalsociety.org/

Sixth Joint Meeting

189th Meeting of the Acoustical Society of America and the Acoustical Society of Japan

Honolulu, Hawaii
1-5 December 2025

Computational Acoustics: Paper 4aSA5

A quantum computing framework for finite-difference time domain and parabolic equation models in ocean acoustics

Noriyuki Kushida
Woods Hole Oceanographic Institution, Woods Hole, MA, 02543, USA; noriyuki.kushida@whoi.edu

Ying-Tsong Lin
Scripps Institution of Oceanography, University of California San Diego, La Jolla, CA, 92093, USA; ytlin@ucsd.edu

Numerical models are essential for investigating and understanding the physics and sound propagation and scattering, given the ocean's complexity and the limitations of real-world field experiments. High-performance computing has become a primary tool for researchers to simulate long-range sound propagation. Quantum computing is an emerging technique that offers potential speedups over conventional binary computers. However, classical algorithms cannot be directly implemented in quantum systems due to fundamental differences in computing principles. This necessitates the development of quantum ocean acoustic models that remain interpretable within the same context as classical algorithms. This paper presents a quantum formulation for a finite-difference time-domain (FDTD) solver and a parabolic equation (PE) method. The results demonstrate that these quantum algorithms implemented on a simulator reproduce results identical to their classical counterparts, providing a foundation for further developments in quantum-centric ocean acoustics.

Proceedings of Meetings on Acoustics, Vol. 60, 022003 (2026); https://doi.org/10.1121/2.0002281.

1. INTRODUCTION

Numerical modeling of ocean acoustics is essential for applications ranging from sonar performance prediction to marine mammal monitoring and environment characterization and exploration. However, as the demand for high-resolution simulations in large-scale environments grows, classical methods such as the Finite-Difference Time-Domain (FDTD) and the Parabolic Equation (PE) method face significant challenges due to the ”curse of dimensionality,” where computational costs scale polynomially or exponentially with the system size. While High-Performance Computing (HPC) techniques have provided acceleration,[1,2] the fundamental scaling limitations remain a bottleneck for global-scale modeling domain.

Quantum computing offers a paradigm shift for solving such wave propagation problems. By leveraging the principles of quantum superposition, interferences and entanglement, Hamiltonian simulation algorithms allow for the unitary evolution of wave functions with a complexity that scales polylogarithmically with the system dimension. Several pioneering works have explored this potential in the time domain. For instance, Costa et al.[3] and Suau et al.[4] investigated general wave equation solvers, while Schade et al.[5] introduced a concept for 1-D elastic waves. More recently, Sato et al.[6] established a rigorous framework for hyperbolic partial differential equations using dual-basis encoding.

Despite these advances in general time-evolution algorithms, applying them to practical underwater acoustics remains non-trivial. Accurate modeling requires rigorous handling of boundary conditions and spatially varying material properties. While abstract operator-based approaches exist, they often struggle to incorporate the specific discretization schemes used in trusted classical solvers, such as the Ghost Node method.

In this paper, we address this gap in two distinct ways. First, for the Time-Domain Wave Equation, we propose a formulation based on Explicit Hamiltonian Construction. While quantum time-evolution itself is not new, the proposed approach focuses on the direct integration of classical assets. By constructing the sparse Hamiltonian matrix directly from the finite-difference stencil, we ensure a one-to-one physical correspondence with classical FDTD solvers. This enables the rigorous implementation of the Ghost Node method on a quantum computer, ensuring that boundary physics are handled with the same fidelity as classical standards.

Second, and perhaps more significantly, we introduce a quantum simulation framework for the Parabolic Equation (PE) method. To the best of our knowledge, this represents the first application of quantum Hamiltonian simulation to the PE method for long-range underwater acoustics. By exploiting the mathematical equivalence between the range-evolution of the acoustic field and the time-dependent Schrödinger equation, we demonstrate that long-range propagation through heterogeneous ocean environments (e.g., the Munk profile) can be efficiently simulated on quantum computers.

By presenting these two complementary approaches, a rigorous boundary-handling scheme for the time domain and a novel quantum solver for the parabolic wave equation, we provide a comprehensive pathway for the next generation of ocean acoustic modeling.

2. TWO-DIMENSIONAL TIME EVOLUTION ACOUSTIC SIMULATION

In this section, we present the formulation and simulation of acoustic wave propagation in a two-dimensional domain. We propose a mapping of the classical wave equation onto a quantum Hamiltonian and validate its accuracy against a classical FDTD solver. Special attention is given to the boundary conditions and the energy-based state mapping to ensure physical consistency between the two computational paradigms.

A. METHODOLOGY

Our formulation builds upon the quantum algorithm originally proposed for one-dimensional elastic wave simulation.[5] However, extending this approach to the two-dimensional acoustic wave equation with specific boundary conditions requires a distinct construction of the spatial operators. Therefore, we provide a detailed derivation of the Hamiltonian and the discretization scheme below.

i. Governing Equations and Hamiltonian Mapping

We consider the scalar acoustic wave equation in a linear medium:

$$\frac{\partial^2 p}{\partial t^2} = \kappa \nabla \cdot (\rho^{-1} \nabla p), \tag{1}$$

where $p(x, y, t)$ is the pressure field, ρ is the mass density, and $\kappa = \rho c^2$ is the bulk modulus (c being the speed of sound).

To implement this on a gate-based quantum computer, we rewrite the second-order PDE as a system of first-order differential equations in the Schrödinger form:

$$\frac{d}{dt} |\psi(t)\rangle = -iH |\psi(t)\rangle . \tag{2}$$

The formal solution to Eq. (2) for a time-independent Hamiltonian is given by $|\psi(t)\rangle = e^{-iHt} |\psi(0)\rangle$. This formulation allows us to map the entire acoustic propagation physics onto the unitary evolution of a quantum state.

ii. Hamiltonian Simulation via Trotterization

The implementation of the unitary operator $U(t) = e^{-iHt}$ requires decomposing the Hamiltonian into a form compatible with quantum gates. We first decompose the Hermitian matrix H into a linear combination of Pauli strings $\{P_j\}$:

$$H = \sum_j c_j P_j, \tag{3}$$

where $P_j \in \{I, X, Y, Z\}^{\otimes n}$ and c_j are real coefficients.

For the time evolution, we employ the first-order Suzuki-Trotter decomposition, which could be considered initially from the exponential operator splitting proposed by Strange in 1968,[7] to approximate the exponential of the sum of non-commuting operators:

$$e^{-iH\Delta t} \approx \prod_j e^{-ic_j P_j \Delta t} + \mathcal{O}(\Delta t^2). \tag{4}$$

Each term $e^{-ic_j P_j \Delta t}$ is then mapped to a standard sequence of quantum gates, consisting of CNOT gates and single-qubit rotations. This approach ensures that the high-dimensional spatial interactions of the acoustic field are efficiently simulated within the Hilbert space of the n-qubit system.

iii. Quantum-Physical Mapping via Energy Normalization

A critical step in our formulation is the mapping between the physical state variables and the quantum state vector $|\psi\rangle$. Unlike classical vectors which can have arbitrary norms, the quantum state evolution is unitary and preserves the L^2 norm ($||\psi||^2 = 1$). To make this compatible with the physics of wave

propagation, we must construct $|\psi\rangle$ such that its norm corresponds to the *total mechanical energy* of the system.

For an acoustic system, the total energy density $\mathcal{E}$ is the sum of kinetic and potential energies. To map this to the quantum probability amplitude, we introduce the energy-normalized variables based on the velocity vector $\mathbf{v}$ and pressure p:

$$\psi_v = \sqrt{\rho}\mathbf{v}, \quad \psi_p = \frac{1}{\sqrt{\kappa}}p. \tag{5}$$

With this transformation, the Euclidean norm of the vector $\boldsymbol{\psi} = [\psi_p, \psi_v]^T$ becomes directly proportional to the physical energy. This normalization is essential for ensuring that the resulting Hamiltonian H is Hermitian even in heterogeneous media.

iv. Hamiltonian Construction and Cholesky Decomposition

In the general case of heterogeneous media, the material parameters ρ and κ become spatial matrices. Following the approach of Schade et al.,[5] we employ an analytical Cholesky decomposition of these material property matrices to symmetrize the wave equation.

By defining the change of variables using the Cholesky factors (e.g., $M = L_\rho L_\rho^T$), we obtain a symmetric Hamiltonian structure. For our specific case of a homogeneous medium discretized on a uniform grid, these factors reduce to scalar coefficients. The resulting Hamiltonian H is constructed as a block skew-Hermitian matrix (multiplied by i):

$$H = i \begin{bmatrix} 0 & cD^T \\ -cD & 0 \end{bmatrix}, \tag{6}$$

where D is the spatial differentiation operator defined below.

v. Boundary Conditions: The Ghost Node Method

A key challenge in comparing quantum and classical grid-based simulations is the consistent implementation of boundary conditions. We employ Dirichlet boundary conditions ($p = 0$ at boundaries) using the *Ghost Node Method*.

The spatial differentiation operator D is crucial for encoding these conditions. Since we simulate a 2D grid, D is constructed from 1D difference operators using the Kronecker product. Let $D_{1\mathrm{D}}$ be the finite difference matrix acting on a 1D domain of size N. To implement the Ghost Node method, $D_{1\mathrm{D}}$ is defined as an $(N+1) \times N$ sparse matrix:

$$D_{1\mathrm{D}} = \frac{1}{\Delta x} \begin{bmatrix} 1 & 0 & \cdots & 0 \\ -1 & 1 & \ddots & \vdots \\ 0 & \ddots & \ddots & 0 \\ \vdots & \ddots & -1 & 1 \\ 0 & \cdots & 0 & -1 \end{bmatrix}. \tag{7}$$

The first row represents the gradient at the left boundary, $(p_0 - p_{\text{ghost}})/\Delta x$, where the ghost node p_{ghost} is implicitly set to zero. Similarly, the last row represents the right boundary. The full 2D operator is $D = [I_N \otimes D_{1\mathrm{D}}; D_{1\mathrm{D}} \otimes I_N]$. This structure ensures that the Laplacian $\nabla^2 \approx -D^\dagger D$ correctly incorporates the zero-boundary conditions at all edges.

vi. Classical Benchmark (FDTD)

As a benchmark for validation, we utilize the classical FDTD method with a central difference scheme (Leap-frog integration). To ensure a rigorous comparison, the discrete Laplacian in the FDTD solver is implemented to strictly match the Hamiltonian's Ghost Node logic defined in Eq. (7). Boundary terms in the Laplacian stencil reference the zero-valued ghost nodes rather than forcing the boundary pixels to zero. This ensures that both simulation methods operate on physically identical effective domains.

B. NUMERICAL EXPERIMENTS

We performed simulations on a 16×16 Cartesian grid ($N = 16$) with parameters $c = 1.0$, $\rho = 1.0$, and grid spacing $\Delta x = 1.0$. The total dimension of the system vector is $2N^2 = 512$, which maps to a 9-qubit system. Note that it will require 65,536 bits in a double precision on a classic computer system to perform the computation. This leads to nearly 7,280 times more fundamental units of information compare to a quantum computer.

The initial condition was set to a Gaussian pulse centered at grid coordinates $(8.0, 8.0)$ with a standard deviation $\sigma = 1.5\Delta x$. The simulation covered the time range $t \in [0, 12.0]$, which is sufficiently long to observe wave propagation and reflection. For the quantum simulation, we used first-order Trotterization with a dynamic step size to maintain numerical precision.

C. RESULTS AND DISCUSSION

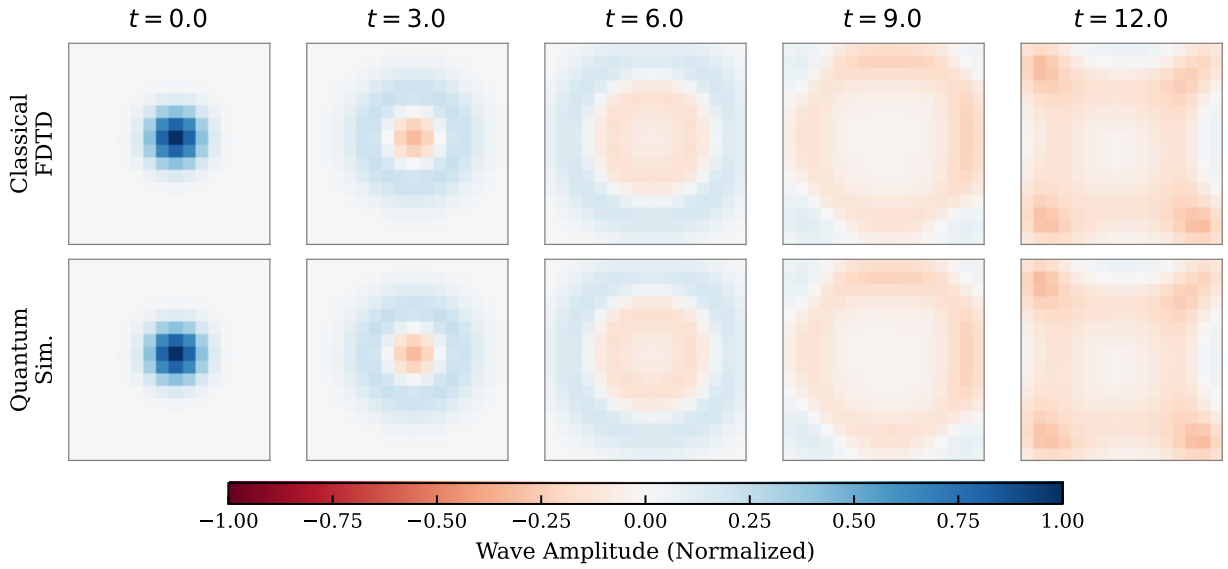

Figure 1: Comparison of 2D Wave Propagation. Top row: Classical FDTD simulation using the Ghost Node method. Bottom row: Quantum simulation result. The snapshots are taken at $t = 0.0, 3.0, 6.0, 9.0, 12.0$***. The wave expands, reflects off the boundaries, and interferes symmetrically, showing excellent agreement between the two methods.***

The comparison between the quantum simulation and the classical FDTD benchmark is visualized in Figure 1 and Figure 2. The time-evolution results demonstrate that:

1. **Propagation Phase** ($t < 6.0$)**:** The wave expands circularly from the center. The quantum simulation perfectly matches the FDTD wavefront velocity and amplitude.

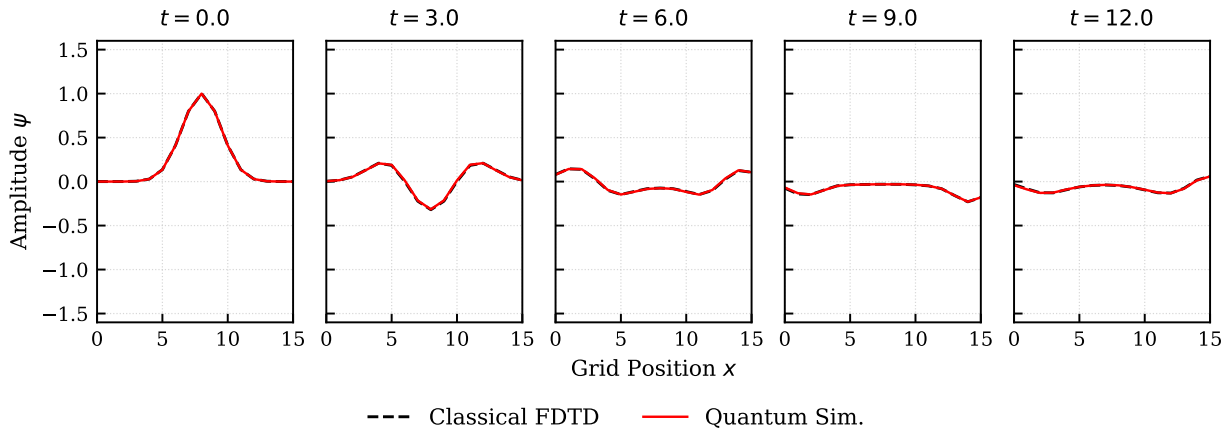

Figure 2: Cross-sectional Amplitude Profiles. Comparison of wave amplitude along the central axis ($y = 8$) ***at corresponding time steps. The quantum simulation (solid red line) accurately tracks the classical benchmark (dashed black line) throughout the propagation and reflection phases.***

2. **Reflection Phase** ($t > 6.0$)**:** The wave reaches the effective boundary defined by the ghost nodes and reflects back toward the center.

Crucially, the interference patterns formed by the reflected waves at $t = 12.0$ show excellent agreement. This confirms that the Hamiltonian encoding with the Ghost Node method correctly captures the physics of the Dirichlet boundary conditions.

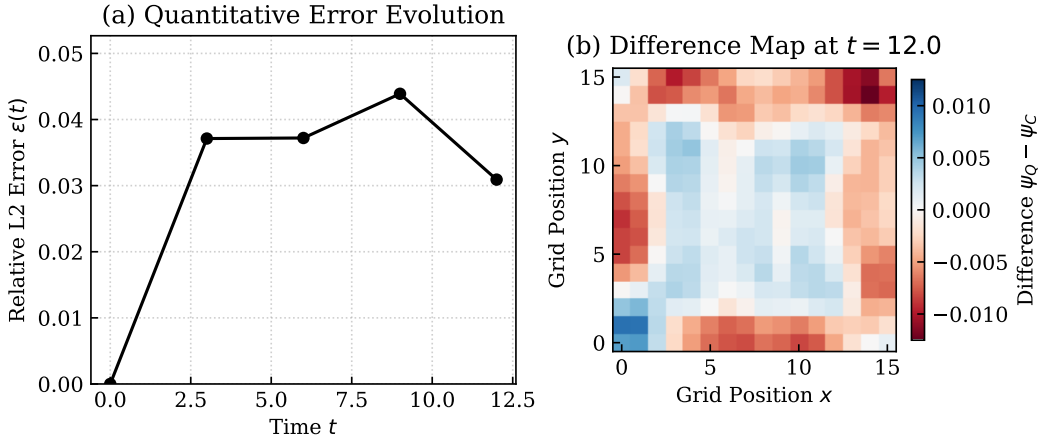

Figure 3: Quantitative Error Analysis. (a) Evolution of the relative L2 error over time. The error grows linearly, which is characteristic of the Trotterization approximation. (b) Spatial distribution of the difference ($\psi_Q - \psi_C$) ***at the final time step*** ($t = 12.0$)***. The error is uniformly distributed without significant bias at the boundaries.***

To further quantify the accuracy, we analyzed the relative L2 error between the quantum state and the classical solution (Figure 3). The error remains low throughout the simulation, increasing linearly due to the accumulation of Trotterization errors. Figure 3(b) displays the spatial distribution of the error at the final time step. The uniform distribution of errors indicates that the Ghost Node implementation introduces no specific artifacts near the boundaries.

3. QUANTUM SIMULATION OF THE PARABOLIC EQUATION

In this section, we present the formulation and simulation of long-range acoustic propagation using the Parabolic Equation (PE) method. Leveraging the analogy between the range-evolution of the acoustic field and the time-evolution of a quantum state, we propose a quantum algorithm based on Hamiltonian simulation.

A. METHODOLOGY

The PE method approximates the Helmholtz equation by assuming one-way propagation, treating the range coordinate r as an evolutionary parameter. This framework allows us to utilize the square root operator formalism to map the acoustic problem onto a quantum mechanical system.

i. Square Root Operator and Narrow-Angle Approximation

Starting from the Helmholtz equation in cylindrical coordinates for the pressure field $p(r,z) = \psi(r,z)H_0^{(1)}(k_0 r)$, the reduced pressure function $\psi(r,z)$ satisfies the far-field wave equation. This can be factored into outgoing and incoming wave components. The equation governing the outgoing wave is expressed using the pseudo-differential square root operator Q:

$$\frac{\partial \psi}{\partial r} = ik_0(Q-1)\psi, \tag{8}$$

where the operator Q is defined as:

$$Q = \sqrt{1 + (n^2(z)-1) + \frac{1}{k_0^2}\frac{\partial^2}{\partial z^2}}. \tag{9}$$

Here, k_0 is the reference wavenumber and $n(z)$ is the refractive index.

To facilitate numerical simulation and mapping to a quantum Hamiltonian, we apply the *narrow-angle approximation*, Tappert's approximation of the square root operator, $Q \approx 1 + q/2$):[8]

$$Q - 1 \approx \frac{1}{2}\left[(n^2(z)-1) + \frac{1}{k_0^2}\frac{\partial^2}{\partial z^2}\right]. \tag{10}$$

Substituting this approximation into Eq. (8) yields the standard narrow-angle parabolic equation:

$$\frac{\partial \psi}{\partial r} = i\left[\frac{1}{2k_0}\frac{\partial^2}{\partial z^2} + \frac{k_0}{2}(n^2(z)-1)\right]\psi. \tag{11}$$

Note that the reason why the narrow-angle approximation is chosen here is to simplify the discussion. Higher order PE approximations can also be utilized.

ii. Quantum Mapping and Hamiltonian Construction

Eq. (11) is mathematically equivalent to the time-dependent Schrödinger equation if we treat the range variable r as the time variable t in the Schrödinger equation:

$$\frac{\partial}{\partial r}|\psi\rangle = -i\hat{H}_{\mathrm{PE}}|\psi\rangle, \tag{12}$$

where the effective Hamiltonian $\hat{H}_{\mathrm{PE}}$ is constructed as:

$$\hat{H}_{\mathrm{PE}} = -\left[\frac{1}{2k_0}\frac{\partial^2}{\partial z^2} + \frac{k_0}{2}(n^2(z)-1)\right]. \tag{13}$$

The solution at range $r + \Delta r$ is given by the unitary evolution operator $|\psi(r+\Delta r)\rangle = e^{-i\hat{H}_{\mathrm{PE}}\Delta r}|\psi(r)\rangle$.

To implement this on a quantum computer, we discretize the depth domain into $N = 2^n$ grid points and decompose the Hamiltonian into Pauli strings, $H \approx \sum_k \alpha_k P_k$. The time-evolution operator is then realized using the Suzuki-Trotter product formula:

$$e^{-iH\Delta r} \approx \prod_k e^{-i\alpha_k P_k \Delta r/2} \cdots \prod_k e^{-i\alpha_k P_k \Delta r/2}. \tag{14}$$

iii. Reference Solution: The Matrix Exponential Method

To rigorously evaluate the accuracy of the quantum simulation, a precise numerical benchmark is required. Standard finite-difference methods, such as the Crank-Nicolson (CN) scheme, rely on rational approximations (e.g., Padé approximants) of the evolution operator, which introduce range-discretization errors.

In contrast, for a range-independent environment where the Hamiltonian matrix $\mathbf{H}$ is constant, the solution can be computed formally as $\boldsymbol{\psi}(r) = \exp(-i\mathbf{H}r)\boldsymbol{\psi}(0)$. The *Matrix Exponential method* computes this matrix exponential directly (e.g., via spectral decomposition or scaling and squaring algorithms) on the discretized spatial grid. This approach eliminates the range-stepping error inherent in finite-difference schemes, providing a "semi-analytical" reference solution that is exact with respect to the range variable.

B. NUMERICAL EXPERIMENTS AND RESULTS

We performed a benchmark simulation of long-range acoustic propagation in a deep ocean environment using the Munk sound speed profile. The simulation parameters were: domain depth $H = 5000$ m, propagation range $r_{\max} = 100$ km, frequency $f = 20$ Hz, and source depth $z_s = 1000$ m. The domain was discretized into $N = 512$ points (9 qubits).

i. Quantum Simulation Performance

To evaluate the fidelity of the proposed quantum algorithm over a long propagation range ($r_{\max} = 100$ km), we performed a direct quantum circuit simulation using the PennyLane quantum software library. The range-stepping operator was implemented using the first-order Trotter-Suzuki decomposition available within the PennyLane framework. For the high-precision simulation, we selected a fine step size of $\Delta r = 0.5$ m.

The simulation was carried out by sequentially applying the quantum circuit block corresponding to the evolution $U(\Delta r)$ to the state vector. This approach allows us to rigorously validate the Trotterization scheme by explicitly capturing the discretization errors inherent in the quantum logic, distinguishing it from standard classical solvers.

Figure 4 presents the comparison of the transmission loss fields. Panel (a) displays the result obtained from the quantum circuit simulation with $\Delta r = 0.5$ m. The interference patterns are visually identical to the Matrix Exponential solution shown in Panel (b), confirming that the chosen Trotter step size effectively suppresses the algorithmic errors.

The accuracy is further validated in Figure 5, which compares the vertical profiles of sound pressure solutions at 100 km. The profile is split into two depth ranges for detailed comparisions: (a) 0–2500 m and (b) 2500–5000 m. The quantum simulation result (black solid line) indeed agrees well with the Matrix

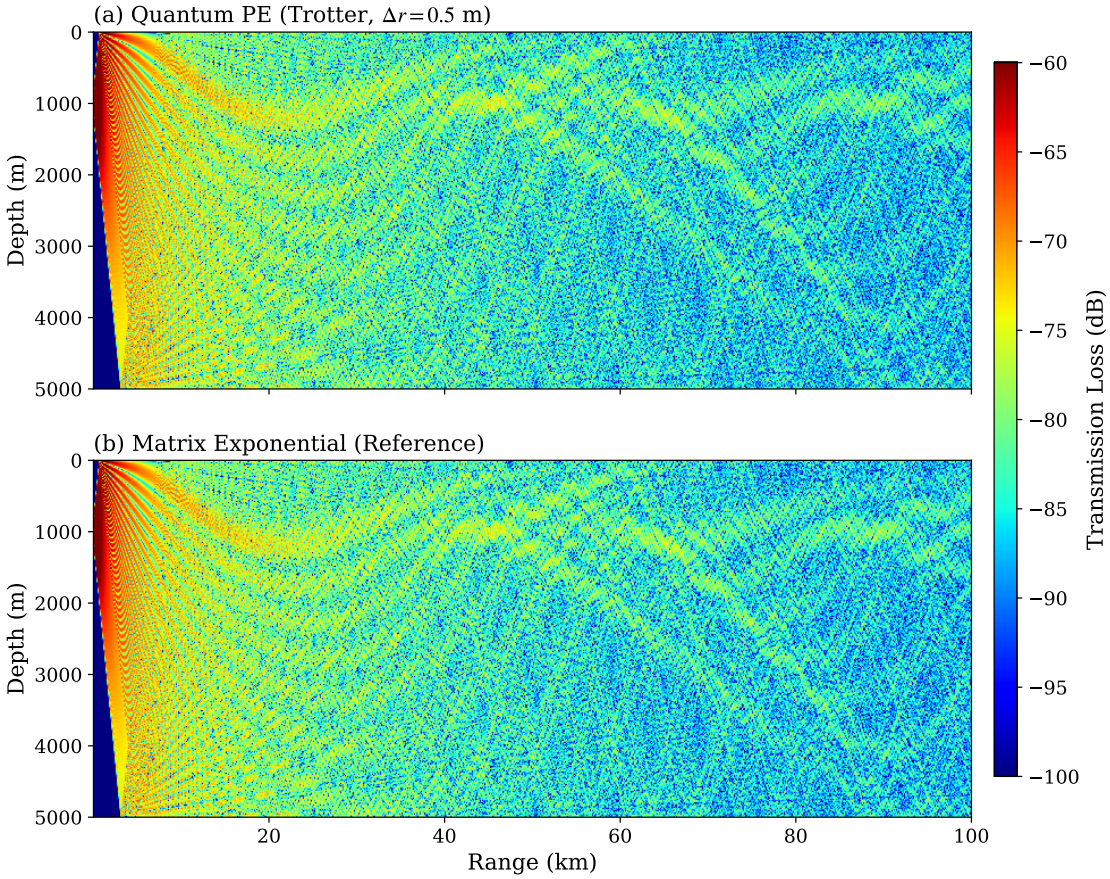

Figure 4: Quantum Simulation Results. (a) TL field computed by the quantum circuit simulation (Trotter decomposition) with a fine step size ($\Delta r = 0.5$ m). (b) Reference field computed by the Matrix Exponential method. The quantum simulation (a) effectively captures the complex interference patterns and matches the reference (b).

Exponential reference (light green thick line). These results demonstrate that the proposed Hamiltonian encoding and Trotterization scheme correctly reproduce the physics of the Parabolic Equation.

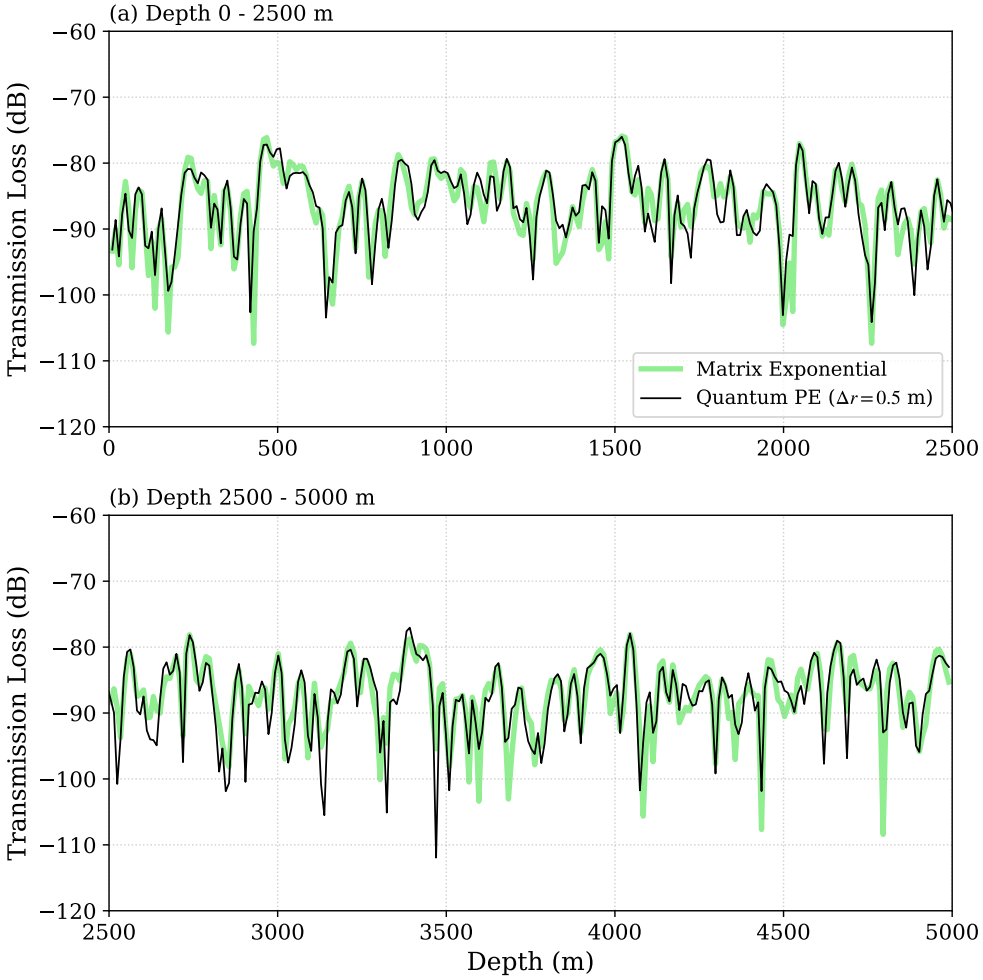

Figure 5: Comparison of Vertical Profiles at 100 km. The profiles are split into two depth ranges: (a) 0–2500 m and (b) 2500–5000 m. The light green thick line represents the Matrix Exponential reference, while the black solid thin line shows the result from the quantum circuit simulation ($\Delta r = 0.5$ m). The agreement confirms the validity of the quantum algorithm.

4. SUMMARY AND OUTLOOK

In this work, we have presented a comprehensive framework for simulating ocean acoustic propagation on quantum computers, explicitly addressing the domain-specific challenges of boundary conditions and long-range transmission. We developed and validated two distinct quantum algorithms: (1) a time-domain solver utilizing a real-space Ghost Node method to strictly enforce Dirichlet boundary conditions at the sea surface, overcoming the limitations of Fourier-based spectral methods; and (2) a Parabolic Equation solver that treats range as a time-like evolution parameter, enabling efficient simulation of propagation through heterogeneous environments like the Munk sound speed profile.

Our numerical benchmarks demonstrate that these quantum algorithms can accurately reproduce the fundamental physics of underwater acoustics. The time-domain simulation matched classical FDTD re-

sults for waveguide scattering, while the quantum PE solver exhibited convergence to the rigorous Matrix Exponential reference, confirming the fidelity of the Hamiltonian mapping and Trotterization scheme.

These results serve as a foundational proof-of-concept for "Quantum Ocean Acoustics." While current demonstrations rely on classical simulators or small-scale devices, the underlying Hamiltonian simulation algorithms offer polylogarithmic scaling, suggesting that future fault-tolerant quantum computers could handle massive 3D ocean environments that remain intractable for classical supercomputers.

Looking forward, a significant frontier lies in extending these linear frameworks to handle nonlinear acoustic phenomena, such as shock wave propagation or high-intensity sonar dynamics governed by the Westervelt or Burgers equations. A promising pathway towards this goal is the recently proposed "Carleman Linearization + Schrödingerization" (CLS) method.[9] This framework addresses the challenges of nonlinearity and dissipation simultaneously: it linearizes polynomial nonlinear terms via high-dimensional embedding (Carleman Linearization) and maps the resulting dissipative dynamics onto a conservative Hamiltonian system using the Warped Phase Transformation. Given that acoustic nonlinearity predominantly manifests as quadratic pressure terms, which align well with the polynomial basis of Carleman linearization, integrating the CLS technique with our ocean acoustic solvers could enable the efficient quantum simulation of complex, nonlinear wave interactions, further expanding the potential impact of quantum computing in marine science.

ACKNOWLEDGMENTS

Ying-Tsong Lin would like to acknowledge the funding support for the Office of Naval Research via Grants N00014-25-1-2017 and N00014-25-1-2041.

REFERENCES

[1] N. Kushida, Y.-T. Lin, P. Nielsen, and R. Le Bras. Acceleration in acoustic wave propagation modelling using openacc/openmp and its hybrid for the global monitoring system. In *Lecture Notes in Computer Science*. Springer, 2020. doi: 10.1007/978-3-030-49943-3_2.

[2] N. Kushida and Y.-T. Lin. Long-range hydroacoustic propagation modelling schemes on distributed memory parallel computers. *J. Theor. Comput. Acoust.*, 2025. doi: 10.1142/S2591728524500221.

[3] P. C. S. Costa, S. Jordan, and A. Ostrander. Quantum algorithm for simulating the wave equation. *Phys. Rev. A*, 99:012323, 2019.

[4] A. Suau, G. Staffelbach, and H. Calandra. Practical quantum computing: solving the wave equation using a quantum approach. *ACM Trans. Quantum Comput.*, 2:1–35, 2021.

[5] M. Schade, C. Bösch, V. Hapla, and A. Fichtner. A quantum computing concept for 1-d elastic wave simulation with exponential speedup. *Geophys. J. Int.*, 238:321–333, 2024.

[6] Y. Sato, R. Kondo, I. Hamamura, T. Onodera, and N. Yamamoto. Hamiltonian simulation for hyperbolic partial differential equations by scalable quantum circuits. *Phys. Rev. Research*, 6(033246), 2024.

[7] G. Strang. On the construction and comparison of difference schemes. *SIAM Journal on Numerical Analysis*, 5:506–517, 1968.

[8] F. D. Tappert. Parabolic equation method in underwater acoustics. *J. Acoust. Soc. Am.*, 55:S34, 1974.

[9] S. Sasaki, K. Endo, and M. Muramatsu. Hamiltonian simulation for nonlinear partial differential equation by schrödingerization. *arXiv preprint arXiv:2508.01640*, 2025.